PERGAMON

Atmospheric Environment 35 (2001) 2533–2544

ATMOSPHERIC ENVIRONMENT

www.elsevier.com/locate/atmosenv

Eddy flux measurements of methane over the fen "Murnauer Moos", 11°11′E, 47°39′N, using a fast tunable diode laser spectrometer☆

Robert Kormann[a,*], Hans Müller[b], Peter Werle[c]

[a]*Max-Planck-Insitut für Chemie, J.J.-Becher-Weg 27, 55128 Mainz, Germany*
[b]*Eulenacker 19, 22175 Hamburg, Germany*
[c]*Fraunhofer Institut Atmosphärische Umweltforschung, Kreuzeckbahnstr. 19, 82467 Garmisch Partenkirchen, Germany*

Received 2 September 1999; received in revised form 7 August 2000; accepted 21 August 2000

Abstract

Eddy covariance measurements of methane were carried out over the fen "Murnauer Moos" in the south of Germany in order to evaluate the performance of a newly developed eddy covariance measurement system, based on a frequency-modulated tunable diode laser spectrometer as a fast chemical sensor. During a six-day period, an average daytime methane emission of $(5.4 \pm 1.8)\,\mathrm{mg\,CH_4\,m^{-2}\,h^{-1}}$ was measured. We find this value moderate, considering the favorable meteorological and soil conditions for methane emission. Diurnal cycles of the fluxes of methane and carbon dioxide as well as of sensible and latent heat are presented. Results are discussed in terms of relevant micrometeorological quantities, and quality control procedures based on Allan variance and spectral analysis are discussed.

Keywords: TDLAS; Vertical turbulent methane flux; Eddy covariance; Micrometeorology; Stationarity

1. Introduction

Methane is the most abundant organic trace gas in the atmosphere. It plays a major role in the tropospheric chemistry of ozone and the hydroxyl radical (Cicerone and Oremland, 1988). As an important radiative active gas, it is also of increasing interest to greenhouse and climate studies. Model calculations (Lelieveld et al., 1998) indicate a contribution of methane to the radiative forcing of all long-lived trace gases of about 22% ($0.57\,\mathrm{W\,m^{-2}}$) during the last century. The atmospheric methane concentration experienced a dramatic increase especially within the last decades and still does, albeit a significant reduction of the trend was observed within the last 10 years or so (Dlugokencky et al., 1998; Khalil and Rasmussen, 1994), which is mostly assigned to decreased sources. Predictions about the future development of atmospheric methane range from a marginal concentration increase (Dlugokencky et al., 1998) to values of about 2.5 to 2.8 ppmv (Lelieveld et al., 1998; IPCC, 1996), depending on the assumptions about the hydroxyl radical concentrations and the source strengths.

Wetlands contribute about three quarters of all natural methane emissions. Surprisingly, model calculations (Lelieveld et al., 1998) show that estimates of the global source strength based on mass balance are more precise than estimates from direct emission measurements. Therefore, reliable emission measurements for different wetland types are urgently needed. However, it is generally accepted that tropical wetlands, although covering only a minor area, contribute a major part to the global

☆This work was carried out when Robert Kormann and Hans Müller were with Fraunhofer Institut Atmosphärische Um-weltforschung, Garmisch-Partenkirchen.

* Corresponding author.
E-mail address: kormann@mpch-mainz.mpg.de (R. Kormann).

1352-2310/01/$ - see front matter
PII: S1352-2310(00)00424-6

sources owing to their high biological turnover. Boreal wetlands account for the rest owing to their large surface extent, except for a minor fraction stemming from mid-latitude wetlands. Measurements should, therefore, concentrate on boreal and tropical wetlands. But in this study, the vicinity of a measurement site to the research institution was a strong argument favoring the fen site, especially for a campaign focused on instrument evaluation purposes. Nevertheless, the measurements presented here can contribute to improve global source strength estimates.

There are numerous papers and books on the advantages and disadvantages of different flux measurement techniques, see, e.g., Lenschow and Hicks (1989), Businger (1986), Foken et al. (1995) or Stull (1988). Among flux measurement techniques, closed chamber techniques usually probe only a small area, which may not be representative for the given biotope (Johansson and Granat, 1984; Folorunso and Rolston, 1984). Additionally, possible disturbances of the transfer resistances (Lenschow and Hicks, 1989; Sebacher et al., 1983) cannot be satisfactorily characterized, and are therefore a major concern. Micrometeorological techniques avoid these problems (Businger, 1986) but require homogeneity of the measurement area (fetch) and stationary micrometeorological conditions. The outstanding technique within these is eddy covariance. It is the only applicable technique avoiding any micrometeorological parameterization, which usually contains considerable uncertainty. But the main obstacle in the routine field application of the eddy covariance technique for the measurement of trace gas fluxes is the need for fast chemical sensors.

Several studies concerned with eddy covariance measurements of methane use infrared absorption to determine gas concentrations. Hovde et al. (1995) have measured the methane emission of a landfill using a custom-built near-infrared instrument with an open multipass arrangement. Fan et al. (1992) used a Zeeman split He–Ne laser as light source for the methane detection in a closed multipass cell arrangement. However, most authors have used closed single or multipass optical arrangements for mid-infrared lead salt diode laser light absorption, e.g., Verma et al. (1992), Shurpali et al. (1993), Edwards et al. (1994), Suyker et al. (1996), Zahniser et al. (1995) or Hargreaves and Fowler (1998). The latter two use a direct absorption detection scheme, whereas the other instruments use a so-called wavelength-modulation (lock-in technique at the kilohertz-range) detection scheme to improve the instruments detection limit. In the instrument used here (Werle and Kormann, 2001) a high-frequency (about 100 MHz) modulation scheme has been implemented, which allows to combine the benefits of narrow band phase-sensitive detection and rapid scanning (kHz) to improve the signal-to-noise ratio, which in turn leads to high data quality. A detailed discussion of different spectrometer techniques can be found in Werle (1998). Flux detection limit estimates (Kormann et al., 1999) based on the results presented here show that these types of instruments may have the potential for eddy covariance measurements of other trace gas species.

Our research project had as its main goal the development of a fast trace gas sensor suitable for the eddy covariance technique (Kormann, 1997; Werle, 1999; Werle and Kormann, 1999, 2001). The frequency-modulated tunable diode laser spectrometer was first used in a field measurement campaign in the fen "Murnauer Moos" to quantify its methane release. This paper describes the measurements and their results. The technical aspects of the system development are presented in Kormann (1997) and Werle and Kormann (2001). The following section describes the measurement system and other devices in operation, as well as the data evaluation scheme. The third section presents the measurement results.

2. Eddy covariance measurement system and flux data evaluation

2.1. Measurement system

The mechanical layout of the fast devices at the measurement head used for the eddy covariance measurements is shown in Fig. 1. The measurement of the wind vector was performed using an ultrasonic anemometer (Solent Research Ultrasonic Anemometer 1012R2, Gill Instruments Ltd., Lymington, Hampshire, UK). It was operated in the "calibrated uvw" mode; that is, the output was corrected for damping of the wind velocity caused by the anemometer mount using an internal procedure. The speed of sound, also determined by the anemometer, was used to derive the virtual temperature. The measurement interval of the anemometer is fixed at 48 ms by the manufacturer, corresponding to a measurement rate of about 20.8 Hz. Based on Moore (1986), the maximum observable frequency (band limit, 3-dB point) due to sensor line effects and time averaging is about 7 Hz, if a typical average wind velocity for the presented measurements of $3\,m\,s^{-1}$ is assumed. Systematic errors caused by uncertainties in the length of the measurement path (Laubach and Teichmann, 1996) were not accounted for. To avoid an unwanted inclination of the anemometer, the measurement head was equipped with an inclinometer (Model 900-T Biaxial Clinometer, Applied Geomechanics, Santa Cruz, CA, USA), which allows a vertical adjustment within the geopotential. Neither drifts or fluctuations nor relevant inclinations of the measurement head could be detected during operation. Water vapor and carbon dioxide measurements were performed using an open path nondispersive infrared

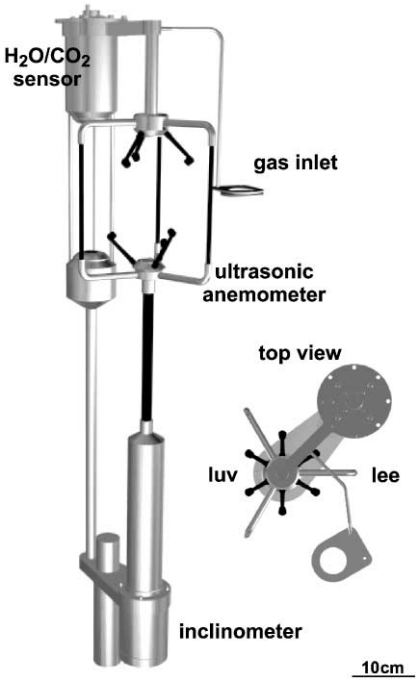

Fig. 1. The measurement head viewed from the preferred wind direction. The nondispersive infrared H_2O/CO_2 sensor and the gas inlet for the spectrometer are mounted behind the measurement paths of the ultrasonic anemometer (see also top view). The inclinometer is positioned below the anemometer mount.

device (Infrared Gas Analyzer Model E009, Advanet Inc., Okayama, Japan). A prototype of this commercial device is described by Othaki and Matsui (1982). Its band limit is found to be about 10 Hz, based again on the approximations of Moore (1986) with an averaging path length of 0.2 m and a wind velocity of $3\,m\,s^{-1}$. The signal of this device was low-pass filtered using a four-pole Butterworth filter (band limit 10 Hz) before it was digitized by the spectrometer.

The diode laser spectrometer is described in detail in Kormann (1997) and Werle and Kormann (2001). The methane concentration is obtained by monitoring the optical absorption of a single ro-vibrational molecular transition at reduced pressure (about 50 hPa) in the mid-infrared (7.9 μm). The laser was housed in a liquid N_2-cryostat (Model L5736, Laser Source Dewar, Laser Photonics Inc., Analytics Division, Bedford, MA, USA); and the beam guided through a multipass cell of the Herriott type (Model 5611, New Focus Inc., Santa Clara, CA, USA) and onto a broad-band MCT detector (SAT, Saint Benoit, France). The laser light source was modulated using a custom built high-frequency signal generator/lock-in arrangement (about 100 MHz) with a single-tone-detection scheme. Dispersive observation with subtle spectra evaluation is used to increase the detectable concentration fluctuations (signal-to-noise ratio) as well as to stabilize the instrument under field conditions, see, e.g., Werle et al. (1994). The band limit of the device was about 2.4 Hz, mainly determined by the gas exchange in the measurement cell, see Kormann (1997) or Werle and Kormann (2001). Since this gas exchange corresponds to a first-order low pass, its frequency characteristics is quite flattish. The measurement interval of the spectrometer was chosen to be 96 ms, in order to easily synchronize the gas concentration measurement with the anemometer data.

To avoid band limiting by large distances between the different measurement devices, the devices were mounted as close as possible to each other, keeping in mind, that a mutual perturbation can be possible. The impacts of the H_2O/CO_2 sensor and the gas inlet onto the wind measurement by shadowing of the wind might be low, since at the height of the wind measurement volume only smaller construction elements are present. A shadowing effect of the additional devices (H_2O/CO_2 sensor, spectrometer gas inlet) is also minimized by downwind mounting from the expected main wind direction (see top view of Fig. 1). Since the gas flow into the inlet of the spectrometer can also cause a nonvanishing wind velocity, the 17-cm distance from the gas inlet to the wind measurement was chosen such that the estimated influence is below the resolution of the anemometer. Based on Moore (1986), Irwin (1979) and Kristensen and Jensen (1979), the separation distances of measurement devices typically should not exeed 10% of the measurement height for unstable stratification and 0.7% of the (positive) Monin–Obukhov length L in the stable case. Since the typical distance in this case is about 15 cm, the measurement height should be above 1.5 m. Values of L between 0 and 21 m during stable stratification were not observed in the described measurement campaign.

The averaging time scale for the turbulent fluxes was chosen to be 30 min (see Businger, 1986), interrupted by a calibration procedure of the diode laser spectrometer (about 20 s). The measurement height z was 6 m, which gives $\bar{u}\,z^{-1} \approx 0.5$ Hz for a typical wind velocity of $3\,m\,s^{-1}$. (For an overview of the notation see the appendix.) This height should allow a thorough observation of the micrometeorologically relevant frequency range, and especially the inertial subrange. Therefore, a test of the measurement system, which was one of the main goals of the campaign, should have been possible. A displacement height was not considered, since the denser vegetation was only about 20-cm tall.

2.2. Data evaluation

The data evaluation splits mainly into three steps: data conditioning, calculation of the fluxes and the spectra, and the calculation of micrometeorological quantities. The data conditioning covers a rotation of the wind

vectors and a trend removal. Four consecutive rotations could be performed on each measured wind vector: a linear rotation in accordance with the instantaneous inclinometer reading; a rotation around the (vertical) z-axis, which makes the horizontal component of the average wind velocity point into positive x-axis; and two linearized rotations causing $\bar{w} = 0$ and $\overline{v'w'} = 0$ (see McMillen, 1988). Only the second rotation is performed on the data shown here, since the others were on average below about one degree. Adopting a systematic error of 3% per degree (Foken et al., 1995), these errors should be kept well below 10%

Trends on the micrometeorological time series, mainly caused by calibration uncertainties of different devices and by micrometeorological instationaries themselves, must be removed before starting any flux calculation. This is usually performed using a running mean or a frequency band limit, both methods being more or less equivalent. However, the determination of the high pass time constant is a problem, and therefore, quantitative means are rare in the literature. In this work we use the Allan variance criterion (Kormann, 1997; Werle et al., 1996; Kramm et al., 1999), which was originally applied to estimate the stability of measurement devices (Werle et al., 1993). It is similar to a stationarity criterion used by Foken and Wichura (1996), but the underlying theory is much more evolved. Stationarity of the micrometeorological time series was typically fulfilled for a hundred to several hundred seconds. Accordingly, the time constant was fixed at 300 s. Tests with several time series indicate a significant decrease of the calculated flux for time constants below 100 s. The uncertainties in the flux results for larger values were well below 10%. An individual detrend in accordance with the Allan variance results for each averaging period was not performed on a routine basis for practical reasons.

A sporadic loss of individual measurement points could occur. These missing values were linearily interpolated from neighboring points. Other data conditioning sometimes found in the literature, as data windowing and despiking (see, e.g., Stull, 1988) was not performed.

For the second step, the calculation of the fluxes, we have to take into account that the instruments used here measure densities (H_2O, CO_2) as well as mixing ratios (CH_4). In accordance to, e.g., Bernhardt and Piazena (1988), we discriminate therefore different flux quantities, termed advective and turbulent flux for the measured densities, and convective and exchange flux for the mixing ratios. Table 1 and Appendix A give a detailed overview about the quantities used here, their notation, and the prerequisites to calculate them.

Pumping the ambient air into the measurement cell of the spectrometer introduces some uncertainty into the simultaneity of time series. Therefore, the calculation of the fluxes is based on the correlation theorem (see, e.g., Press et al., 1988 or Wienhold et al., 1994). The covariance is calculated as a function of the time shift between the time series, and therefore the correct time lag together with the flux can be derived. The standard deviations within the covariance plots for time shifts between 100 and 200 s were used to estimate the measurement error. This method takes into account both, the real (Gaussian) measurement errors of the individual data points and the uncertainty in the stationarity during the averaging time interval. Although not mathematically rigid, this "covariance error measure" turned out to be a very conservative estimate for the errors of the turbulent fluxes. Gaussian error propagation, applied to the turbulent flux, which ignores instationarity in contrast to the covariance error, was found to cause about 10% of the error in the data shown below.

The Fourier-transformed time series were used to derive the relevant spectra and ogives. Cospectra and quadrature spectra, as well as coherence and phase spectra were deduced using the time delay given from the correlation analysis. Exponentially growing frequency bins were formed for the typical logarithmic representation of the spectra. This analysis shows that the considered frequency range between about 0.003 and 5 Hz contained the main contributions to the turbulent fluctuations and fluxes, which is comparable to other micrometeorological findings (Kaimal et al., 1972). No corrections for the band-limiting effects mentioned in the previous section of the measurement devices were performed.

In the final step of the data evaluation, pertinent micrometeorological quantities were derived to complete the micrometeorological description of the experiment. Mainly, these are the average vertical wind velocity $\bar{w}$ to calculate the total fluxes of methane, carbon dioxide and water vapor; the friction velocity u_* and the stability parameter $z\,L^{-1}$; the sensible (H) and the latent (Q) heat fluxes; and the Bowen ratio β. The appendix summarizes the flux quantities, which can be derived from the measured fast time series, and the micrometeorological quantities as used in this study. We estimated the "footprint" of the eddy covariance measurements as discussed by Schuepp (1990). Typically, the estimated relative flux rate maxima were around 50 m upwind of the measurement point.

3. Measurement campaign Murnauer Moos

3.1. Measurement site and meteorological measurement conditions

The measurement site was located within the fen "Murnauer Moos" at a longitude of 11°11′E and a latitude of 47°39′N, which is in southern Germany about 2.5-km south of the town of Murnau. It has an elevation

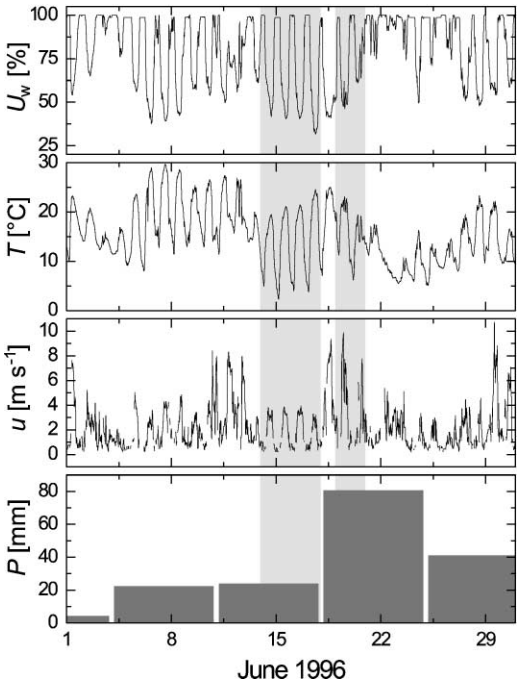

Fig. 2. Meteorological parameters near the measurement site for June 1996. The relative humidity U_w, the air temperature T (at about 4 m above ground) and the wind velocity u are depicted with a time resolution of 30 min. The precipitation P is accumulated for one week. The light grey stripes indicate the two analyzed measurement periods.

of about 622 m above sea level. Owing to valley winds into the nearby Loisach valley, which forms about 10 km S to SW of the measurement site, northerly to northeasterly winds are dominating during daytime at fair weather conditions, accompanied usually by unstable stratification. Southerly mountain winds, often observed during the night, had to be rejected because of violated homogeneity conditions.

Based on the classification scheme given by Roulet and Barrie (1994), the measurement area may be characterized as fen. No soil investigations were performed, but stratigraphical surveys (Döben and Frank, 1983) indicate an approximately 4-m deep peat layer on a quite inhomogeneous gravel and limestone bed. The soil might be enriched by mineral carbon owing to regular flooding from a vast network of ditches and especially from the lime-rich water of the nearby river Loisach. The water pH within the fen is around neutral. The most frequent species of the plant cover are *Primula farinosa*, *Schoenus ferrugineus*, *Phragnutes communis*, *Carex elata* and *Betonica officianalis*. The total annual precipitation in 1996 was 1096 mm, the annual mean temperature 5.3°C.

The analyzed measurement periods are 14–17 June and 19–20 June 1996. Fig. 2 shows meteorological parameters for June 1996 measured nearby. It indicates a very warm period around 8 June. The precipitation was mainly due to some thunderstorms. The first measurement interval falls into a fair weather period having very regular meteorological conditions. A steady increase of the daily air temperatures, which are quite moderate at the beginning, can be seen. The wind velocity is mainly caused by the orography and therefore remarkably regularly. Cloudy and partly rainy days followed with improving weather conditions during the second observation period. A total of 82 half-hour flux measurement intervals (74 for the first and 8 for the second period) were examined. The daily cycle for 16 June will also be shown exemplarily.

The micrometeorological measurements were further accompanied by measurements of the atmospheric pressure, the radiation balance, the soil temperature and its volumetric water content, and the fen surface temperature. The radiation was measured using a Schulze–Lange net radiation sensor (Dr. Bruno Lange GmbH, Berlin, Germany) at about 1.8 m height. A sonde using the principle of time domain reflectometry (TRIME-ES sonde P2, UMS GmbH, München, Germany) was used to estimate the soil volumetric water content in a depth of about 10 cm, where also the soil temperature was measured using a 4-pole Pt 100 sensor. For the fen surface temperature measurements, a pyrocamera system (KT 15.83, Heimann GmbH, Wiesbaden, Germany) was used.

Fig. 3 shows the meteorological conditions of 16 June 1996. The radiation measurements indicate a fair weather summer day with some clouds during the afternoon. The maximum downward radiation was found at 12:16 (noon; given times are local time) to be about 1250 W m^{-2}. At about 18:30, the radiative cooling of the ground sets in with a maximum measured rate of about 45 W m^{-2}. An intercomparison with nearby (25-km south of the site) performed solar radiation measurements (pyranometer) during clear sky conditions showed that the incoming radiation in the thermal spectral range was about 290 W m^{-2}, corresponding to a (blackbody) radiation temperature of 267 K. Assuming an infrared emissivity of 0.93 for grassland (e.g., Stull, 1988), the albedo of the site was found to be 0.21, which is a typical value for grassland reported in the literature. The maximum net radiation was more or less constant at a rate of 625 W m^{-2} during the first interval (14–17 June), whereas there was a slight increase of about 50 W m^{-2} in the maximum incoming and outgoing radiation. Owing to the weather conditions, there was smaller radiation transfer in the second measurement period.

The soil water content at a depth of about 10 cm decreased slightly in the fair weather period from 62 to about 56% with a typical diurnal cycle as shown in Fig. 3. In the second period, it increased again to about 57% owing to the intermediate rainfall. As a result of the

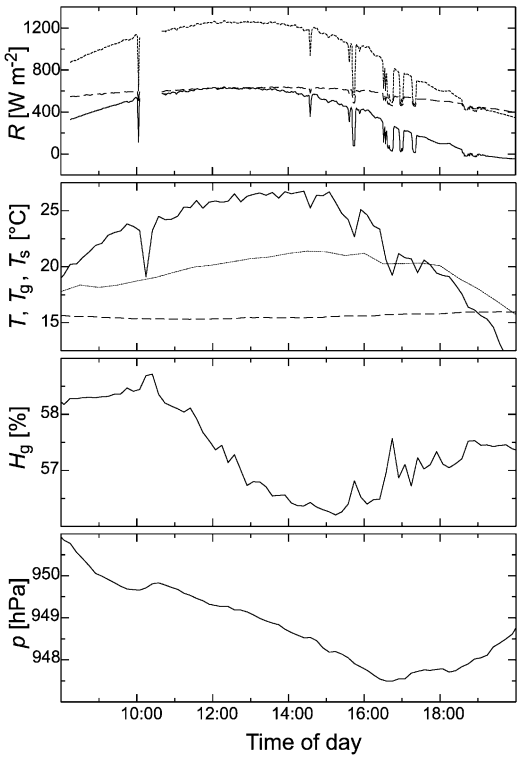

Fig. 3. Meteorological quantities of 16 June 1996. The uppermost graph contains the incoming total radiation (dotted curve), the upward radiation (dashed curve) and the net radiation R (solid curve). The second graph depicts temperatures: the air temperature T (dotted curve), the surface temperature T_s (solid curve) and the soil temperature T_g (dashed curve). The soil water content H_g and the air pressure p complete the figure. For details see text.

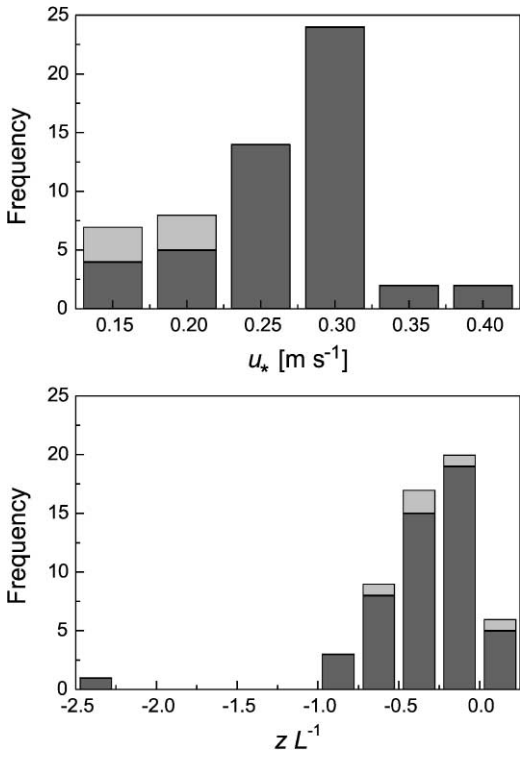

Fig. 4. Histograms of the micrometeorological parameters u_* and $z\,L^{-1}$, split into the fair weather (first) period (dark grey) and the second period (light grey).

reduced irradiation, the diurnal cycle disappeared in the second period. The minimum soil water content typically occurred with a delay of about 3 h after the maximum of the latent heat flux. The maximum soil temperature was reached about 8 h after the maximum solar height. Most of the delay might be caused by the low thermal diffusivity of water, and to a lesser extent it might be due to a shadowing effect of the plant cover. The observed temperatures were around 16°C during the first (fair weather) period. The total variation of the soil temperature during the day is quite low (0.7°C). The local atmospheric pressure gradually decreased in the first period from 954 to 946 hPa. On 20 June a pressure of 936 hPa was measured. These values correspond to normalized pressures in the range from 1008 to 1024 hPa, which confirms the already-mentioned weather conditions for the two measurement periods.

For further interpretation the data had to be preselected in order to meet some specific criteria: the average wind velocity had to exceed a minimum of $0.5\,\mathrm{m\,s^{-1}}$, and the average wind directions should be due to the required homogeneity within northerly directions in the range from 270–360° and 0–60°. For the first measurement period, the average wind velocity was quite constant at $2.9 \pm 0.3\,\mathrm{m\,s^{-1}}$, where the data during the onset and the lulling of the valley wind (typically a half- to one-hour interval with $\bar{u} < 2\,\mathrm{m\,s^{-1}}$) were rejected. Mainly during this fair weather period, the wind came from NE with occasional turns to N. During the second period, a shift to directions from NW was observed, which coincided with a decrease of the wind velocities below $2\,\mathrm{m\,s^{-1}}$. Observed friction velocities u_* were $(0.27 \pm 0.05)\,\mathrm{m\,s^{-1}}$ for the first and $(0.17 \pm 0.03)\,\mathrm{m\,s^{-1}}$ for the second period. Fig. 4 summarizes the observed friction velocities and the stability parameters $z\,L^{-1}$, the latter reflecting the mainly unstable micrometeorological conditions according to the selection criteria.

3.2. Turbulent fluxes and turbulent transfer

The trace gas fluxes of methane and carbon dioxide are shown in Fig. 5 for 16 June. The carbon dioxide uptake, F_k, by the plants clearly shows a diurnal cycle. The methane emission, F_c, might be mainly driven by the soil

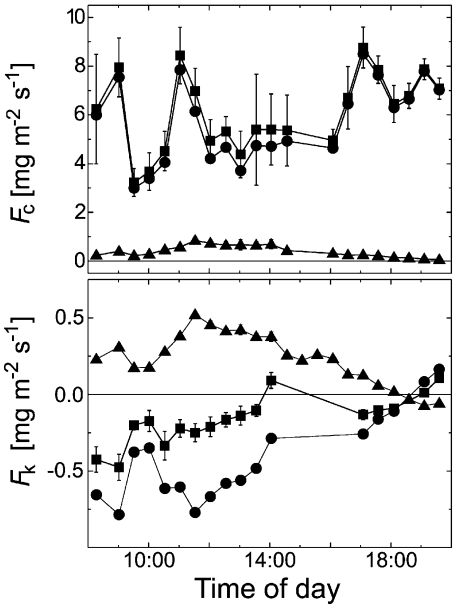

Fig. 5. Diurnal cycle of the fluxes of methane (F_c) and carbon dioxide (F_k) on 16 June. The convective or advective parts of the fluxes (triangles) as well as the total fluxes (squares) are depicted. The non-turbulent fluxes are considerable only in the case of carbon dioxide. Error bars are mostly smaller than the size of the symbols for the advective fluxes, and are not depicted for turbulent fluxes for clarity.

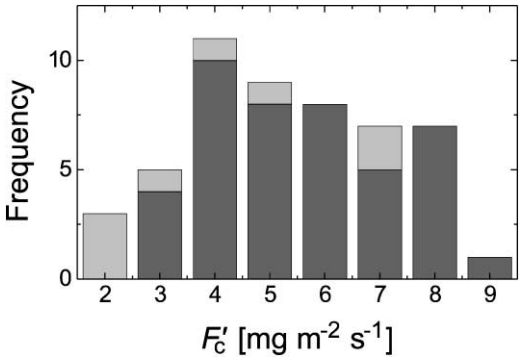

Fig. 6. Histogram of the observed methane fluxes (F_c') over the total measurement period. The dark grey values correspond to the first measurement period, the light grey to the second.

temperature and soil water content and, therefore, shows no pronounced diurnal cycle. However, plant-mediated processes might also influence the emissions to a certain extent. For example, the reduction of the methane flux around 10:00 might be a result of changed micrometeorological conditions (reduced radiation). The advective part (see the appendix) of the carbon dioxide flux as well as the convective part of the methane flux are also depicted. Since its absolute concentration was not measured, only an estimate of the advective carbon dioxide flux can be given here. Assuming an average concentration of 360 ppmv or 0.63 g m^{-3}, we find a considerable contribution to the total carbon dioxide fluxes. Averaged over the whole day, the ratio of the advective to the turbulent fluxes is about -59%. In contrast to this, the contribution of the convective methane fluxes to the total fluxes are marginal. Averaged again over the whole day, the correction of the methane fluxes is about 7% and, therefore, below the statistical error estimated for the exchange flux from the covariance plots. These corrections correspond to an estimated average wind velocity of 0.35 mm s^{-1} for 16 June. The estimated average vertical wind velocity for all analyzed measurement intervals is (0.39 ± 0.21) mm s^{-1}; the fraction of the advective flux from the turbulent flux for carbon dioxide is $-57 \pm 28\%$; and the convective flux from the exchange flux for methane is $7 \pm 5\%$.

The average (downward) carbon dioxide flux during the first measurement period was (-0.83 ± 0.51) g CO_2 m^{-2} h^{-1}. Fig. 6 depicts a histogram of the observed methane fluxes during the total measurement period. The average methane flux is (5.4 ± 1.8) mg CH_4 m^{-2} h^{-1}. The observed values range from 1.7 to 8.9 mg m^{-2} h^{-1}. There is a slight tendency for lower methane fluxes in the second measurement period, which might be due to a changed mean wind direction. A moderate dependence of the turbulent methane flux on the wind direction occurred, with a maximum for northerly directions. We suspect that this is connected to an inhomogeneous water surface caused by a field-path crossing the measurement site.

Several campaign-style eddy covariance measurements of CH_4 with laser-based concentration measurement devices from natural wetlands are published in literature (see, e.g., Verma et al., 1992; Fan et al., 1992; Edwards et al., 1994; Hovde et al., 1995 or Hargreaves and Fowler, 1998). Shurpali et al. (1993) or Suyker et al. (1996) report season-long measurements. Based on several measurements over fens, Aselmann and Crutzen (1989) estimated an average emission of 3.3 mg CH_4 m^{-2} h^{-1}. Our results fit well into their range of 1.2–9.0 mg m^{-2} h^{-1}, although being somewhat higher than the average. However, considering the favorable methane production conditions (eutrophic and pH neutral peat conditions at high humidity and temperature), we find our observed methane fluxes quite moderate. For example, Verma et al. (1992) found comparable to slightly higher CH_4 fluxes within a site at the same latitude, although there the peat conditions are more acidic and therefore less preferable for methanogenesis. Although it is highly speculative, two different observations could be responsible for this. Firstly, the measurement area is usually flooded several times a year by the nearby river Loisach, which certainly brings

in nutrients but which primarily seems to be responsible for a quite high mineral carbon content of the upper layers of the fen. Besides that, a continuous population development of methanogenic bacteria seems to be impossible because of the flooding, especially because methanogens are expected to grow slowly (Segers, 1998). Secondly, the measurement area is mowed every year in autumn to prevent bushes and trees from growing for natural preservation purposes, and the cut is harvested. This might cause a limitation of the organic carbon substrate for the microorganisms (Segers, 1998).

Shurpali et al. (1993), measuring at the site of Verma et al. (1992) over one growing season, confirm their results, being also somewhat higher than the measurements reported here. No indication of flux increases correlated to the air pressure, as observed there, could be seen in our measurements; but this might be due to the shorter measurement period. A 30% increase of the fluxes during the first measurement period was observed, which coincides with an air pressure reduction of about 10 hPa, but which might be due to several other reasons. However, no obvious correlation could be observed with other meteorological data as soil temperature and water content (which varied only very little), surface temperature or net radiation. The fluxes of Suyker et al. (1996), measuring a somewhat more northerly fen with comparable neutral pH, vary from similar values up to a factor of 3 higher at comparable peat temperature, confirming the suspicion of moderate emissions from our site. Although being highly speculative, we would not expect a major increase of emissions during the further growing season, based on air temperature considerations. Consequently, a flux of $6\,\mathrm{mg\,CH_4\,m^{-2}\,h^{-1}}$ might be an upper boundary for the emissions. Taking a growing season of 6 months and the size of this small fen (1500 ha), we find a total emission of about $400\,\mathrm{t\,CH_4\,a^{-1}}$. Long-term measurements would lead to a more representative result, but we are not aware of such measurements.

As an example of a diurnal cycle, the sensible and the latent heat fluxes for 16 June 1996 are shown in Fig. 7. Owing to the fair weather conditions, a pronounced daily cycle can be observed. The net radiation R together with the measurements of the sensible (H) and the latent heat fluxes (Q) (Fig. 8a) allows the solution of the energy balance equation $R - G = H + Q$ for the soil heat flux G, which should be quite low owing to the wet soil conditions. There might be a slight calibration uncertainty in the radiation data (R slightly too low), but in general the observations reflect a closed balance. Appreciable soil heat fluxes appear only when the net radiation and therefore the heating of the surface is high. Generally, only a small fraction of the incident energy flux is converted into soil heat flux, occasionally reaching about half. The Bowen ratio β is depicted in Fig. 8b. The line within the graph corresponds to $\beta = 0.3$, which is typical for wetlands (Stull, 1988).

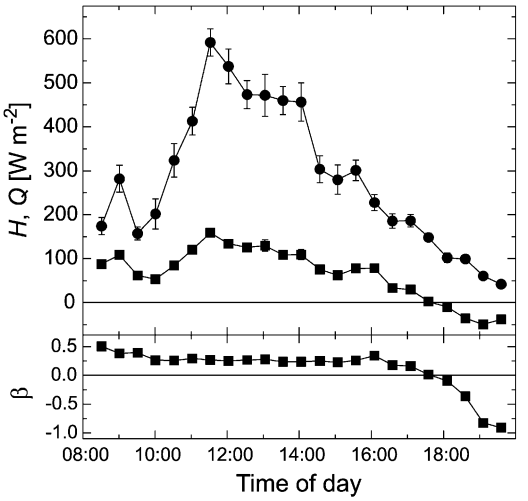

Fig. 7. Diurnal cycle of the sensible and latent heat fluxes H (squares) and Q (circles). Typical for wetlands is the large fraction of latent heat flux during unstable stratification, corresponding to a low Bowen ratio β.

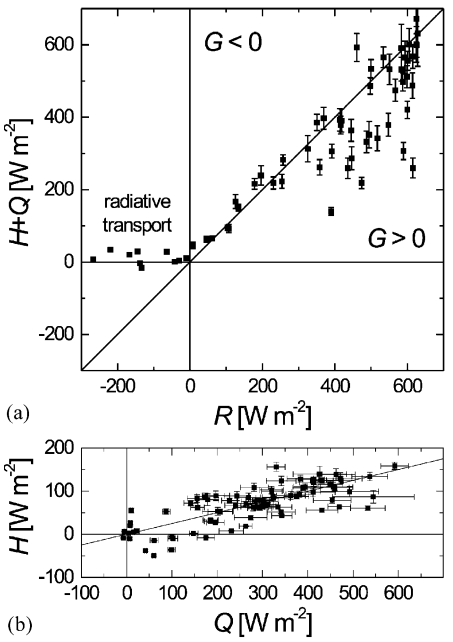

Fig. 8. (a) The energy balance for the total measurement period. The low soil heat flux is typical for the wet soil conditions. (b) Sensible heat flux H versus latent heat flux Q, from which the Bowen ratio β can be deduced. The line corresponds to a Bowen ratio of 0.3.

The development of the turbulent CO_2 flux with increasing net radiation (Fig. 9) shows the expected saturation curve, despite the fact that net radiation is only a rough estimate for the photosynthetically active

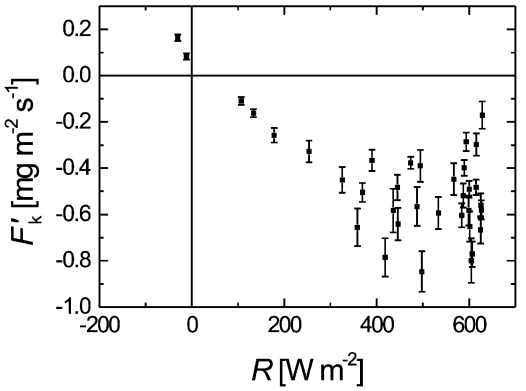

Fig. 9. A typical saturation curve for the plant's carbon dioxide uptake. Assuming an albedo of 0.21 and a fraction of 30% of the solar radiation being photosynthetically active, the saturation value corresponds to a PAR of about 1.4 mmol m^{-2} s^{-1}.

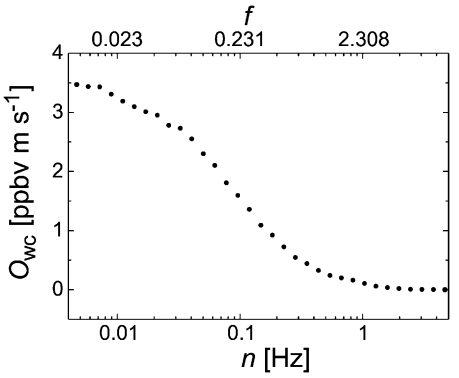

Fig. 11. The ogive for the cospectrum depicted in Fig. 10. A thorough recording of all relevant flux portions can be seen clearly.

radiation (PAR) relevant here. Regardless, a saturation point around 500 W m^{-2} corresponds to a photosynthetically active radiation of 1.4 mmol m^{-2} s^{-1}, assuming 30% of the solar irradiation photosynthetically active and using the above estimated albedo of 0.21. This corresponds well with values given in the literature (Larcher, 1973).

Spectra allow quality control of eddy covariance data. An example of spectra, the cospectrum and the coherence spectrum for 16 June, 19:06 is shown in Fig. 10. The inertial subrange with its $n^{-5/3}$ behavior can clearly be seen within the spectra of the vertical wind and methane. The cross within the graph of the vertical wind marks the expected position of the maximum within the energy containing range (Kaimal et al., 1972). The cospectrum shows the accepted $n^{-7/3}$ behavior. The corresponding ogive (Fig. 11), which is the integral representation of the cospectrum, shows that the relevant frequency range is completely covered.

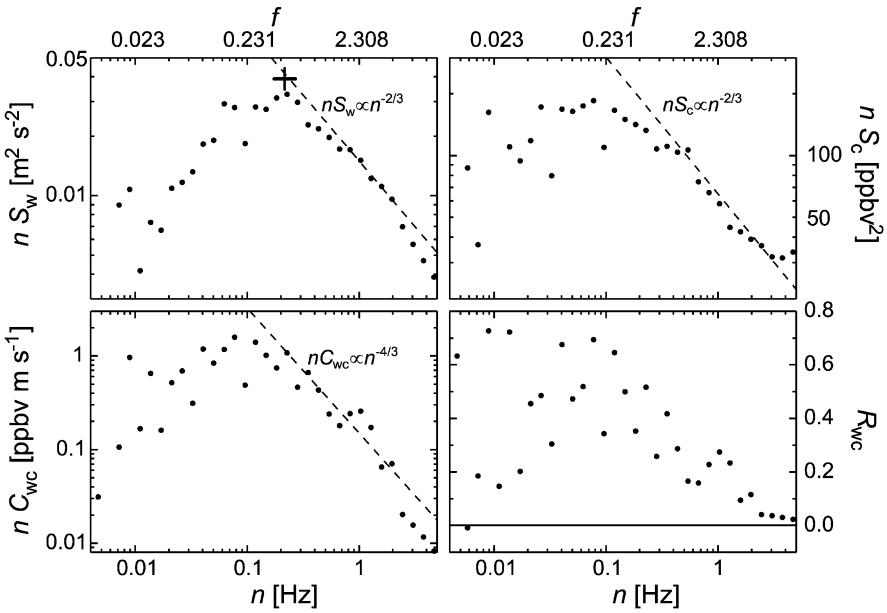

Fig. 10. Spectra, the cospectrum and the coherence spectrum for the turbulent methane flux during stable atmospheric stratification (16 June, 19:06). The power is decreasing in the inertial subrange as expected. The cross within the spectrum of the vertical wind marks the maximum given by Kaimal et al. (1972). For the notation see the appendix, $f = nz/\bar{u}$ is the normalized frequency.

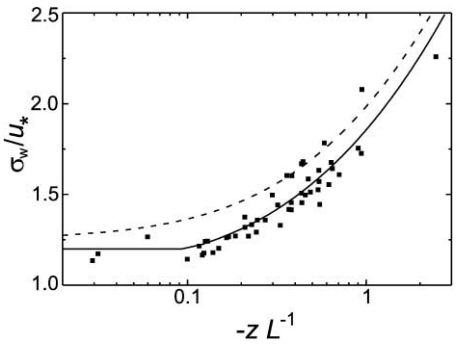

Fig. 12. The normalized standard deviations of the vertical wind. The solid line depicts the model of Andreas (1995), the dashed line the one of Panofsky et al. (1977). As expected the results show that the downwind obstacles do not seriously influence the vertical turbulence.

A further quality control, the normalized standard deviations of the vertical wind for the unstable cases, is displayed in Fig. 12. The intercomparison with two different empirical relationships given by Andreas (1995) (solid line) and by Panofsky et al. (1977) (dashed line) shows that downwind obstacles present at the site do not seriously influence the turbulent vertical wind field at the measurement point.

4. Summary and concluding remarks

We presented eddy covariance measurements of methane above the fen Murnauer Moos, which is located close to the Bavarian Alps in the south of Germany. The mean daytime methane flux derived from 30-min sampling intervals during the measurement period was $(5.4 \pm 1.8)\,\mathrm{mg\,CH_4\,m^{-2}\,h^{-1}}$. We consider this value as a moderate emission, keeping the favorable methane production conditions in mind. For quality control purposes the spectra and ogives were analyzed and it was confirmed that the results are well within theoretical expectations concerning the spectral behavior, especially in the high-frequency domain. The inertial subrange with its $n^{-5/3}$ behavior can clearly be seen within the spectra of the vertical wind and methane. This confirms that the new fast chemical sensor based on high-frequency modulated tunable diode laser spectroscopy in the mid-infrared region is capable to resolve atmospheric trace gas turbulent fluctuations up to 5 Hz, based on a 10 Hz sampling rate. A new type of stability measure based on the Allan variance criterion was used to estimate an adequate time constant for the high-pass filtering of the fast micrometeorological time series. During data analysis, the data were preselected to fulfill specific criteria with respect to minimum horizontal wind speed and wind direction in order to ensure the fetch requirements. To complete the picture and for a comprehensive description of the field experiment, meteorological parameters were recorded and fluxes of latent and sensible heat were determined to evaluate the energy balance. Additionally, carbon dioxide and humidity fluxes were determined. The Bowen ratio β, friction velocity u_*, stability parameter $z\,L^{-1}$, and the distance of maximum flux contribution derived from the sensor footprint were carefully analyzed to assure the quality of the micrometeorological trace gas flux measurements based on the eddy covariance technique. The newly

Table 1
Overview of the most important quantities

Quantity		Derived from
Methane exchange flux	F_c''	$w', c', \bar{\rho}$
Turbulent H_2O/CO_2 flux	$F'_{q,k}$	$w', \rho'_{q,k}$
Turbulent flux of T_v	F'_T	w', T'_v
Momentum flux	F'_u	u', w'
Convective methane flux	$\langle F_c \rangle$	$F'_q, F'_T, \bar{\rho}, \bar{\rho}_q, \bar{c}$
Average wind velocity	$\bar{w}$	$F'_q, F'_T, \bar{\rho}, \bar{\rho}_q$
Advective H_2O flux	$\bar{F}_q$	$\bar{w}, \bar{\rho}_q$
Friction velocity	$u_* = \sqrt{-F'_u}$	
Stability parameter	$z\,L^{-1} = -\frac{\kappa g}{\bar{T}_v}\frac{zF'_T}{u_*^3}$	g gravitational constant z measurement height $\kappa = 0.4$ von-Kármán constant
Turbulent heat flux	$\overline{w'T'} \approx \overline{w'T'_v} - k\overline{w'\rho'_q}$	$k \approx 0.16\,\mathrm{K\,m^3\,g^{-1}}$ (depending on T_v and ambient pressure)
Sensible heat flux	$H = c_p\overline{w'T'}$	$c_p = 1004.7\,\mathrm{J\,K^{-1}\,kg^{-1}}$ (specific heat of dry air at constant pressure)
Latent heat flux	$Q = l\overline{w'\rho'_q}$	$l = (3145.5 - 2.36\bar{T}_v\mathrm{K^{-1}})\,\mathrm{J\,g^{-1}}$ (latent heat of evaporization)
Bowen ratio	$\beta = H/Q$	

developed diode-laser-based fast chemical sensor applied here has proven to be well suited for eddy covariance measurements.

Acknowledgements

We thank the Umweltbundesamt for the long-term weather data (Fig. 2) and the Landratsamt Garmisch-Partenirchen for the information about the plant habitat at the measurement site. We have to acknowledge the fruitful comments of the referees, as well as the careful proofreading of the manuscript by Dr. Carol Strametz.

Appendix A. survey of most important quantities and their notation

The ultrasonic anemometer was used to determine the wind components u, v, w ($\bar{u} > 0, \bar{v} = 0$) and the virtual temperature T_v. The trace gas devices used within the described campaign measure densities or mass per volume for water vapor, ρ_q, and CO_2, ρ_k, as well as CH_4 mixing ratios, $c = \rho_c/\rho$, with respect to moist air. We distinguish therefore the advective flux $\bar{F}_{q,k} = \bar{w}\overline{\rho_{q,k}}$, the convective flux $\langle F_c \rangle = \bar{\rho}\bar{w}\bar{c}$, the turbulent flux $F'_{q,k} = \overline{w'\rho'_{q,k}}$ and exchange flux $F''_c = \bar{\rho}\overline{w'c'}$, describing the advective and the turbulent part of the respective total fluxes $F_{q,k} = \bar{F}_{q,k} + F'_{q,k}$ and $F_c = \langle F_c \rangle + F''_c$ (see, e.g., Bernhardt and Piazena, 1988). We corrected for the correlated density effects (Webb et al., 1980) postulating $F_a = \overline{\rho_a w} = 0$ (ρ_a dry air density). Cospectra C_{gh} of the time series $g(t)$ and $h(t)$ are defined as $C_{gh}(f) = \Re e[G(f)H^*(f)]$ with G and H as the Fourier transforms of the corresponding time series. These are normalized to yield $\overline{gh} = \int_0^\infty C_{gh}\,\mathrm{d}f$. Spectra $S_g = C_{gg}$ designate the special case $g = h$. The coherence spectrum is defined by $R_{gh} = C_{gh}(S_g S_h)^{-1/2}$. The ogive O_{gh} is the integrated cospectrum from a certain frequency f to infinity.

Table 1 summarizes the most important quantities and their notation used in this work.

References

Andreas, E.L., 1995. Statistics of surface layer turbulence and evaluations of eddy-accumulation coefficients. Proceedings of the Eleventh Symposium on Boundary Layers and Turbulence, Charlotte, NC, 27–31 March 1995, p. 106.

Aselmann, I., Crutzen, P.J., 1989. Global distribution of natural freshwater wetlands and rice paddies, their net primary productivity, seasonality and possible methane emissions. Journal of Atmospheric Chemistry 8, 307.

Bernhardt, K., Piazena, H., 1988. Zum Einfluß der turbulenzbedingten Dichteschwankungen auf die Bestimmung turbulenter Austauschströme in der Bodenschicht (On the influence of turbulence related density fluctuations on the determination of turbulent fluxes within the boundary layer). Zeitschrift für Meteorologie 38, 234.

Businger, J.A., 1986. Evaluation of the accuracy with which dry deposition can be measured with current micrometeorological techniques. Journal of Climate and Applied Meteorology 25, 1100.

Cicerone, R.J., Oremland, R.S., 1988. Biogeochemical aspects of atmospheric methane. Global Biogeochemical Cycles 2 (4), 299.

Dlugokencky, E.J., Masarie, K.A., Lang, P.M., Tans, P.P., 1998. Continuing decline in the growth rate of the atmospheric methane burden. Nature 393, 447.

Döben, K., Frank, H., 1983. Geologische Karte von Bayern, Erläuterungen zum Blatt Nr. 8333 Murnau (Comments on geological maps of Bavaria). Bayerisches Geologisches Landesamt, München.

Edwards, G.C., Neumann, H.H., den Hartog, G., Thurtell, G.W., Kidd, G., 1994. Eddy correlation measurements of methane fluxes using a tunable diode laser at the Kinosheo Lake tower site during the Northern wetlands study (NOWES). Journal of Geophysical Research D 99, 1511.

Fan, S.M., Wofsy, S.C., Bakwin, P.B., Jacob, D.J., Anderson, S.M., Kebabian, P.L., McManus, J.B., Kolb, C.E., Fitzjarrald, D.R., 1992. Micrometeorological measurements of CH_4 and CO_2 exchange between the atmosphere and the subarctic tundra. Journal of Geophysical Research D 97, 16627.

Foken, T., Dlugi, R., Kramm, G., 1995. On the determination of dry deposition and emission of gaseous compounds at the biosphere–atmosphere interface. Meteorologische Zeitschrift N.F. 4, 91.

Foken, T., Wichura, B., 1996. Tools for quality assessment of surface-based flux measurements. Agricultural and Forest Meteorology 78, 83.

Folorunso, O.A., Rolston, D.E., 1984. Spacial variability of field-measured denitrification gas fluxes. Soil Science Society of America Journal 48, 1214.

Hargreaves, K.J., Fowler, D., 1998. Quantifying the effects of water table and soil temperature on the emission of methane from peat wetland at the field scale. Atmospheric Environment 32, 3275.

Hovde, D.C., Stanton, A.C., Meyers, T.P., Matt, D.R., 1995. Methane emissions from a landfill measured by eddy correlation using a fast response diode laser sensor. Journal of Atmospheric Chemistry 20, 141.

Intergovernmental Panel on Climate Change (IPCC), 1996. In: J.T. Houghton et al. (Eds.), Climate Change 1995: The Science of Climate Change. Cambridge University Press, Cambridge, UK.

Irwin, H.P.A.H., 1979. Cross-spectra of turbulence velocities in isotropic turbulence. Boundary-Layer Meteorology 16, 237.

Johansson, C., Granat, L., 1984. Emission of nitric oxide from arable land. Tellus 36B, 25.

Kaimal, J.C., Wyngaard, J.C., Izumi, Y., Coté, O.R., 1972. Spectral characteristics of surface-layer turbulence. Quarterly Journal of the Royal Meteorological Society 98, 563.

Khalil, M.A.K., Rasmussen, R.A., 1994. Trends of atmospheric methane. Pure & Applied Chemistry 66 (1), 137.

Kormann R., 1997. Entwicklung eines frequenzmodulierten Diodenlaserspektrometers zur Bestimmung von Spurengasflüssen in der Atmosphäre (Development of a

frequency-modulated diode laser spectrometer for the determination of trace gas fluxes in the atmosphere). IFU-Schriftenreihe Bd. 49/97, 1. Aufl. 1997.

Kormann, R., Fischer, H., Wienhold, F.G., 1999. A compact multi-laser TDLAS for trace gas flux measurements based on a micrometeorological technique. SPIE Proceedings 3758, 162.

Kramm, G., Beier, N., Dlugi, R., Müller, H., 1999. Evaluation of conditional sampling methods. Contributions to Atmospheric Physics 72, 161.

Kristensen, L., Jensen, N.O., 1979. Lateral coherence in isotropic turbulence and in the natural wind. Boundary-Layer Meteorology 17, 353.

Larcher W., 1973. Ökophysiologie der Pflanzen (Ecophysiology of plants). Verlag Eugen Ulmer Stuttgart, 5. Aufl. 1994, pp. 394.

Laubach, J., Teichmann, U., 1996. Measuring energy budget components by eddy correlation: data corrections and application over low vegetation. Beiträge zur Physik der Atmosphäre 69 (2), 307.

Lelieveld, J., Crutzen, P.J., Dentener, F.J., 1998. Changing concentration, lifetime and climate forcing of atmospheric methane. Tellus 50B, 128.

Lenschow, D.H., Hicks, B.B., 1989. Global tropospheric chemistry – chemical fluxes in the global atmosphere. Workshop Report, NCAR, Boulder.

McMillen, R.T., 1988. An eddy correlation technique with extended applicability to non-simple terrain. Boundary-Layer Meteorology 43, 231.

Moore, C.J., 1986. Frequency response corrections for eddy correlation systems. Boundary-Layer Meteorology 37, 17.

Othaki, E., Matsui, T., 1982. Infrared device for simultaneous measurement of fluctuations of atmospheric carbon dioxide and water vapor. Boundary-Layer Meteorology 24, 109.

Panofsky, H.A., Tennekes, H., Lenschow, D.H., Wyngaard, J.C., 1977. The characteristics of turbulent velocity components in the surface layer under convective conditions. Boundary-Layer Meteorology 11, 355.

Press, W.H., Teukolsky, S.A., Vetterling, W.T., Flannery, B.P., 1988. Numerical Recipes. Cambridge University Press, Cambridge.

Roulet, N.T., Barrie, L.A., 1994. Methane emissions from Northern wetlands: source strength and uncertainties in estimates. Pure & Applied Chemistry 66 (1), 170.

Schuepp, P.H., Leclerc, M.Y., McPherson, J.I., Dejardins, R.L., 1990. Footprint prediction of scalar fluxes from analytical solutions of the diffusion equation. Boundary-Layer Meteorology 50, 355.

Sebacher, D.I., Harriss, R.C., Bartlett, K.B., 1983. Methane flux across the air–water interface: air velocity effects. Tellus 35B, 103.

Segers, R., 1998. Methane production and methane consumption: a review of processes underlying wetland methane fluxes. Biogeochemistry 41, 23.

Shurpali, N.J., Verma, S.B., Clement, R.J., Billesbach, D.P., 1993. Seasonal distribution of methane flux in a Minnesota peatland measured by eddy correlation. Journal of Geophysical Research D 98, 20649.

Stull, R.B., 1988. An Introduction to Boundary Layer Meteorology. Kluwer Academic Publishers, Dordrecht.

Suyker, A.E., Verma, S.B., Clement, R.J., Billesbach, D.P., 1996. Methane flux in a Boreal fen: season-long measurement by eddy correlation. Journal of Geophysical Research D 101, 28637.

Verma, S.B., Ullman, F.G., Billesbach, D., Clement, R.J., Kim, J., Verry, E.S., 1992. Eddy correlation measurements of methane flux in a Northern peatland ecosystem. Boundary-Layer Meteorology 58, 289.

Webb, E.K., Pearman, G.I., Leuning, R., 1980. Correction of flux measurements for density effects due to heat and water vapor transfer. Quarterly Journal of the Royal Meteorological Society 106, 85.

Werle, P., 1998. A review of recent advances in semiconductor laser based gas monitors. Spectrochimica Acta 54A, 197.

Werle, P., 1999. Laseroptical sensors for in-situ gas analysis. Recent Research Developments in Optical Engineering 2, 124.

Werle, P., Kormann, R., 1999. Measurements of trace gas fluxes using tunable diode laser spectroscopy. SPIE Proceedings 3821, 124.

Werle, P., Kormann, R., 2001. A fast diode-laser sensor for eddy correlation measurements of methane emissions from rice paddy fields. Applied Optics 40, 846–858.

Werle, P., Kormann, R., Mücke, R., Foken, Th., Kramm, G., Müller, H., 1996. Analysis of time series data: a time domain stability criterion for stationarity tests. Proceedings EUROTRAC 96. Vol. 2, p. 703.

Werle, P., Mücke, R., Slemr, F., 1993. The limits of signal averaging in atmospheric trace-gas monitoring by tunable diode-laser absorption spectroscopy. Applied Physics B57, 131.

Werle, P., Scheumann, B., Schandl, J., 1994. Real time signal-processing concepts for trace-gas analysis by diode-laser spectroscopy. Optical Engineering 33 (9), 3093.

Wienhold, F.G., Frahm, H., Harris, G.W., 1994. Measurements of NO_2 fluxes from fertilized grassland using a fast response tunable diode laser spectrometer. Journal of Geophysical Research D 99, 16557.

Zahniser, M.S., Nelson, D.D., McManus, J.B., Kebabian, P.L., 1995. Measurement of trace gas fluxes using tunable diode laser spectroscopy. Philosophical Transactions of the Royal Society London A 351, 371.